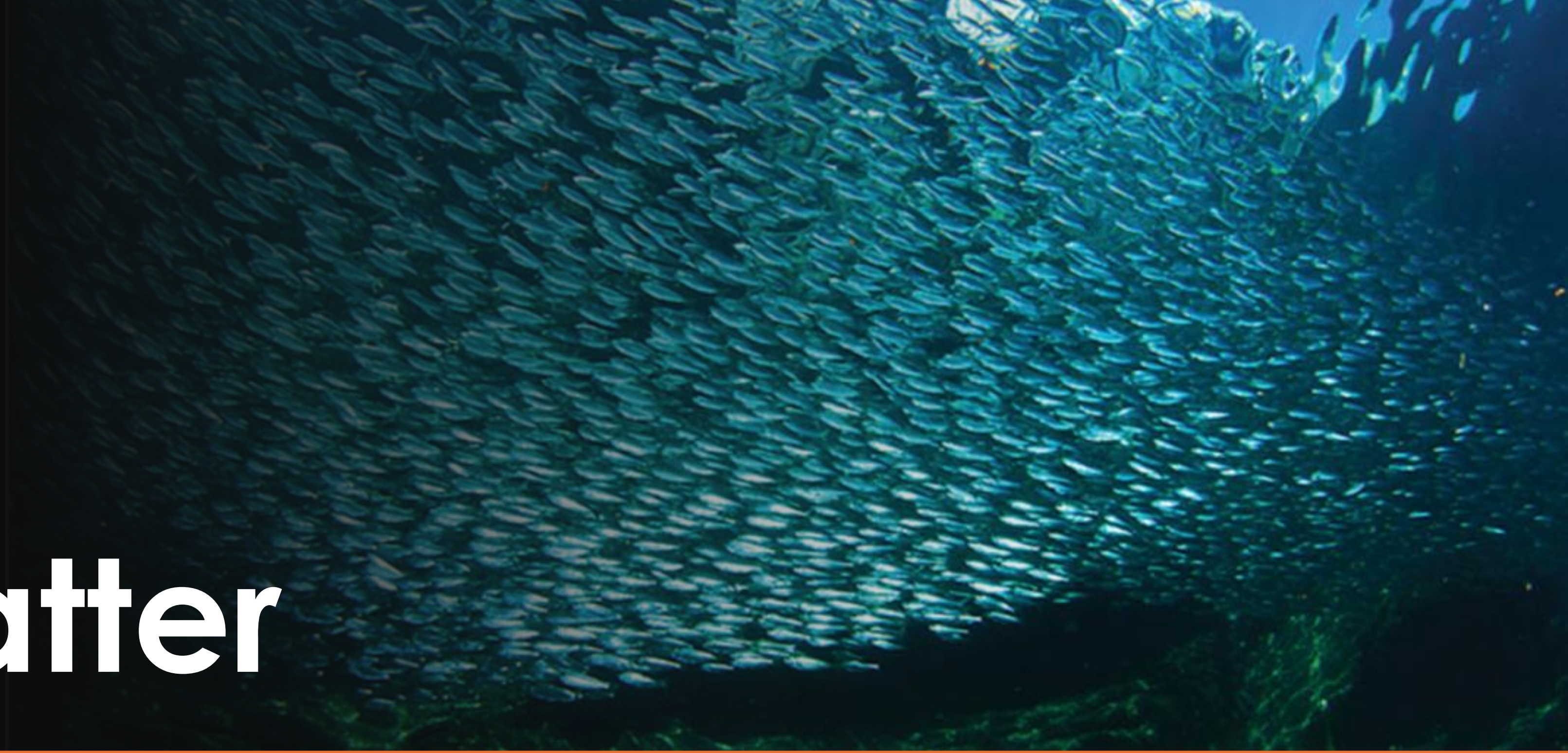

Active Matter

Flocking, Self-propelled, Chiral & Chemotactic

Boids Model

Simulated Flocks

- **Collision Avoidance**:
  avoid collisions with nearby flockmates
- **Velocity Matching:**
  attempt to match velocity with nearby flockmates
- **Flock Centering:**
  attempt to stay close to nearby flockmates

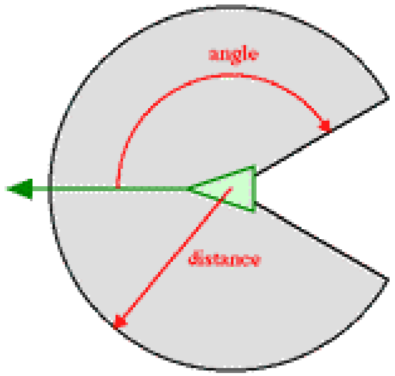

a boid's neighborhood

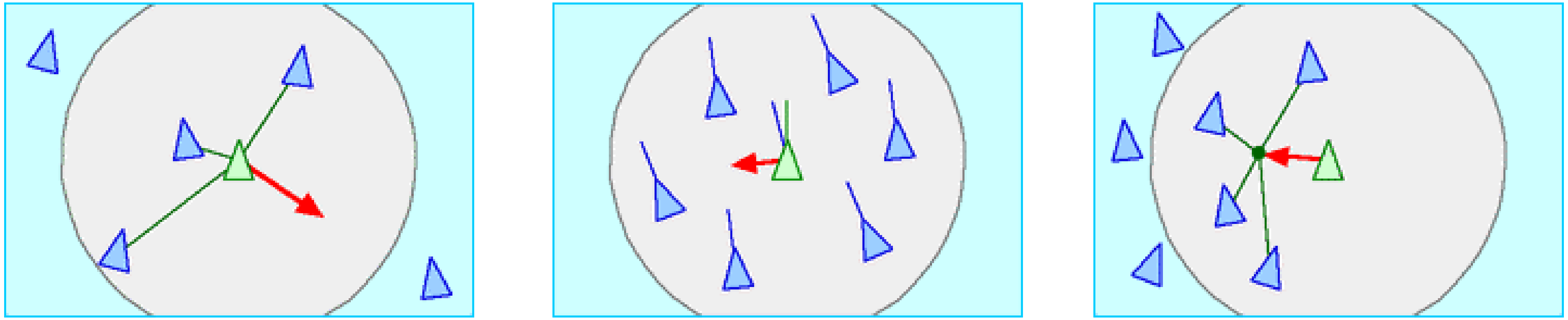

J. Toner and Y. Tu, Flocks, Herds, and Schools: A Quantitative Theory of Flocking, Phys. Rev. E 58, 4828 (1998).

C. W. Reynolds, Flocks, Herds, and Schools: A Distributed Behavioral Model, Computer Graphics 21, 25 (1987).

Vicsek Model

$$\mathbf{x}_i(t+1) = \mathbf{x}_i(t) + \mathbf{v}_i(t)\Delta t\ ,$$
$$\theta(t+1) = \langle \theta(t) \rangle_r + \Delta\theta\ .$$

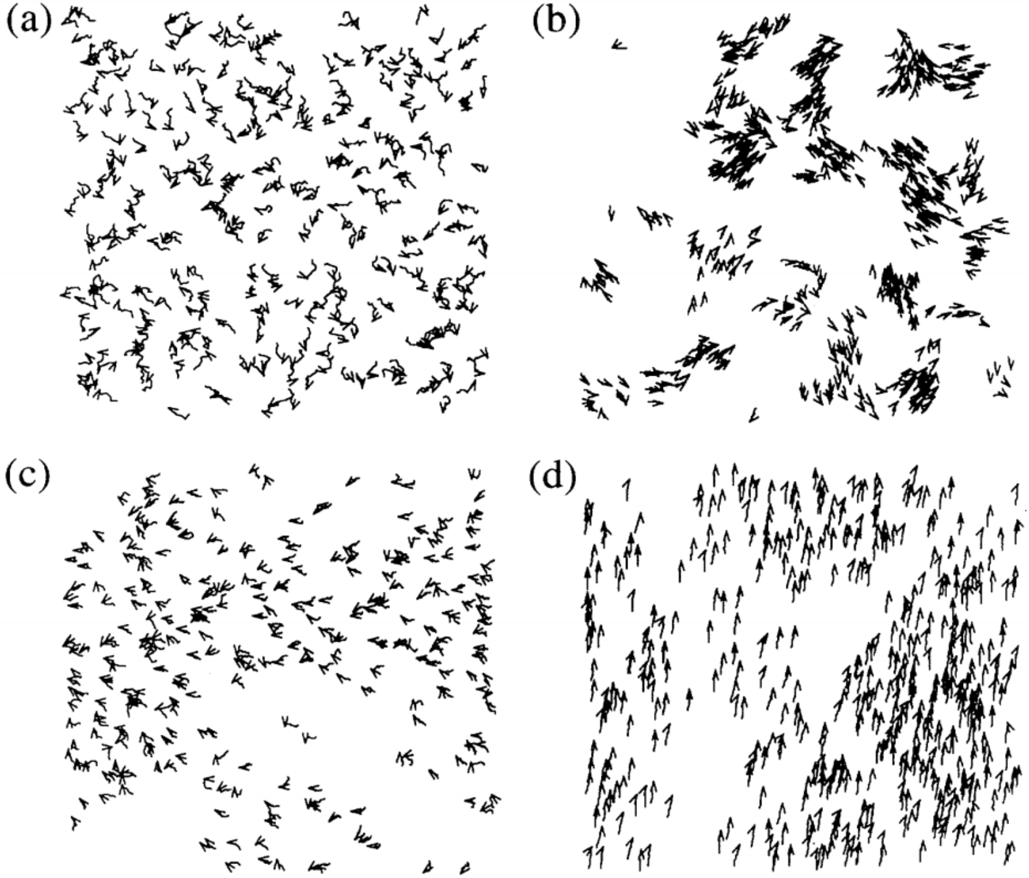

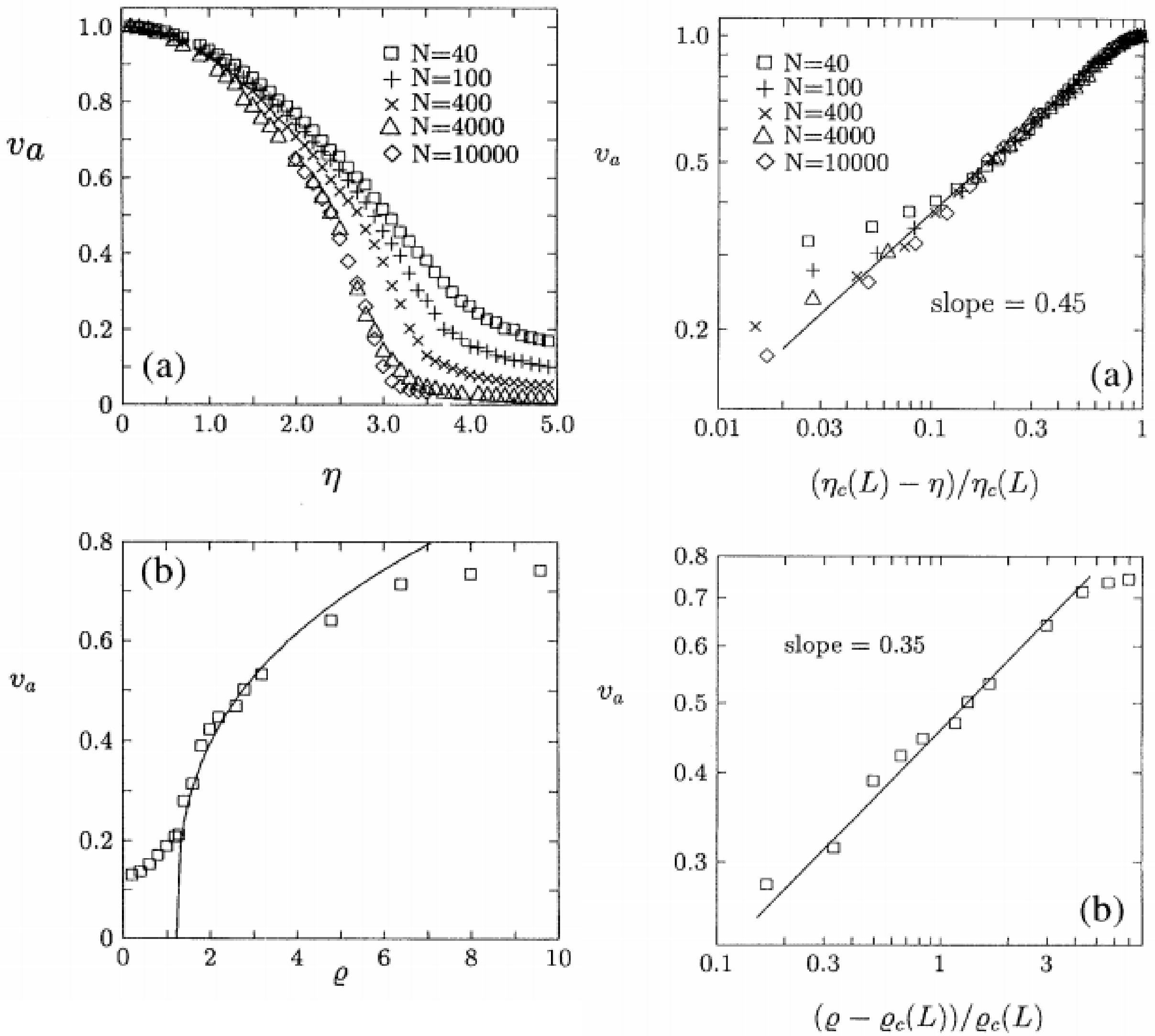

T. Vicsek, A. Czirók, E. Ben-Jacob, I. Cohen, and O. Shochet, Phys. Rev. Lett. 75, 1226 (1995).

Self-Propelled Particles

$$\dot{r}_i = c\,\mathbf{e}_{\theta_i}$$

$$\dot{\theta}_i = \gamma \sum_{j=1}^{N} F\left(\theta_j - \theta_i, r_j - r_i\right) + \sqrt{2\epsilon}\,\tilde{\boldsymbol{\eta}}_i(t),$$

$$F(\theta, r) = \begin{cases} \dfrac{\sin(\theta)}{\pi R^2}, & |r| < R \\ 0, & \text{otherwise} \end{cases}$$

$$f(\mathbf{r}, \theta) = \sum_{j==1}^{N} \delta(\mathbf{r} - r_j)\,\delta(\theta)$$

$$\partial_t f(\mathbf{r}, \theta) + \mathbf{e}_\theta \cdot \nabla[vf]$$
$$= \epsilon \frac{\partial^2 f}{\partial \theta^2} - \frac{\partial}{\partial \theta}\sqrt{2\epsilon f}\,\boldsymbol{\eta} - \gamma \frac{\partial}{\partial \theta}\int d\theta' d\mathbf{r}' f(\mathbf{r}', \theta')$$
$$\times f(\mathbf{r}, \theta) F(\theta' - \theta, \mathbf{r} - \mathbf{r}').$$

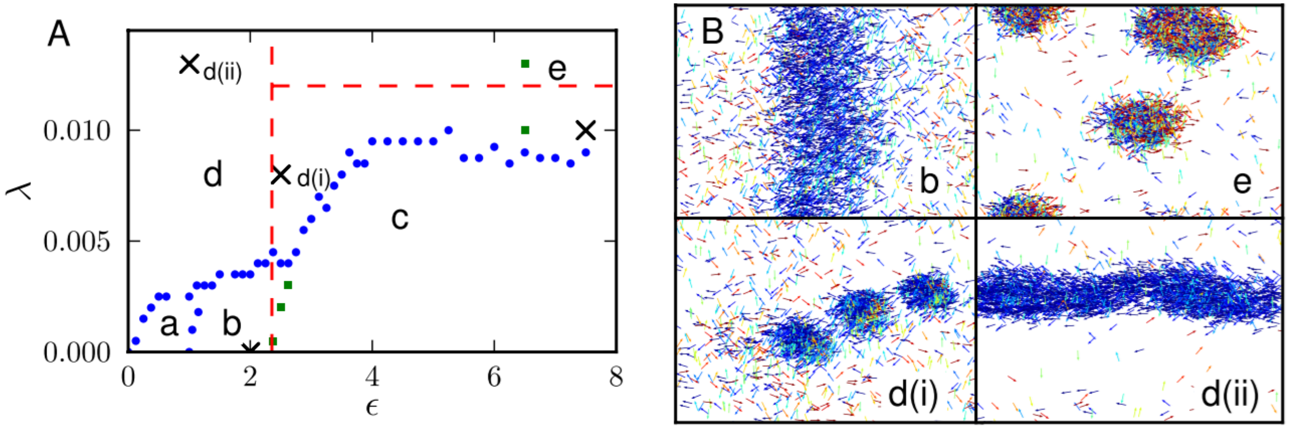

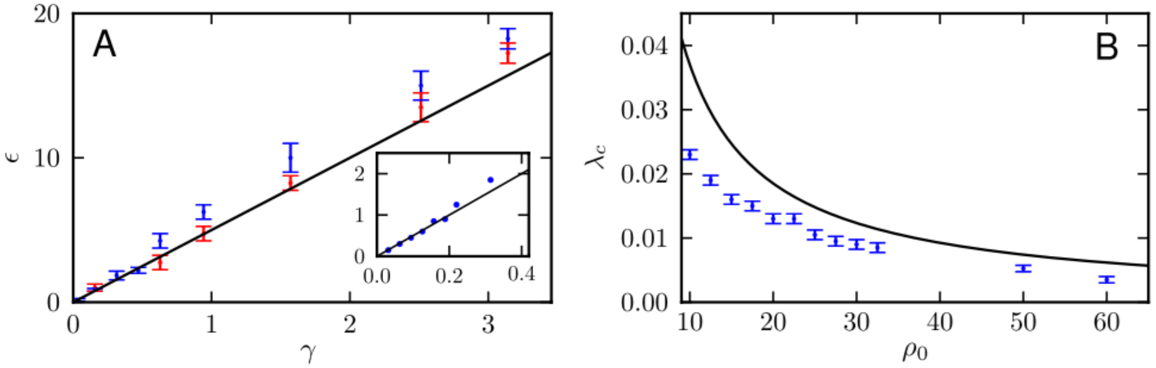

FIG. 2 (color online). (a) Phase boundary for the flying XY model when $\lambda = 0$, showing the critical value of ϵ as a function of γ. Blue (darker gray) points for $v = 2.0$, red (lighter gray) for $v = 0.5$. Inset: data for $v = 2.0$ for smaller values of γ. (b) Phase boundary for $\epsilon = 5$, $\gamma = 0.16$. In all cases $L = 10$ and $N = 1000$.

CAPs Model

$$\dot{\mathbf{r}}_i = v\mathbf{p}_i,$$

$$\dot{\theta}_i = \omega + \frac{K}{\pi R_\theta^2}\sum_{j\in\partial_i}\sin(\theta_j - \theta_i) + \sqrt{2D_r}\eta_i, \qquad (1)$$

$$\dot{\rho} = -\mathrm{Pe_r}\nabla\cdot\mathbf{w}, \qquad (2)$$

$$\begin{aligned}\dot{\mathbf{w}} = &(g\rho - 2)\frac{\mathbf{w}}{2} - \frac{\mathrm{Pe_r}}{2}\nabla\rho + \frac{\mathrm{Pe_r^2}}{2b}\nabla^2\mathbf{w} - \frac{g^2}{b}|\mathbf{w}|^2\mathbf{w}\\ &+ \frac{g\mathrm{Pe_r}}{4b}[5\nabla\mathbf{w}^2 - 10\mathbf{w}(\nabla\cdot\mathbf{w}) - 6(\mathbf{w}\cdot\nabla)\mathbf{w}]\\ &+ \Omega\mathbf{w}_\perp + \frac{\mathrm{Pe_r^2}\Omega}{4b}\nabla^2\mathbf{w}_\perp - \frac{g^2\Omega}{2b}|\mathbf{w}|^2\mathbf{w}_\perp\\ &- \frac{g\mathrm{Pe_r}\Omega}{8b}[3\nabla_\perp\mathbf{w}^2 - 6\mathbf{w}(\nabla_\perp\cdot\mathbf{w}) - 10(\mathbf{w}\cdot\nabla_\perp)\mathbf{w}]. \qquad (3)\end{aligned}$$

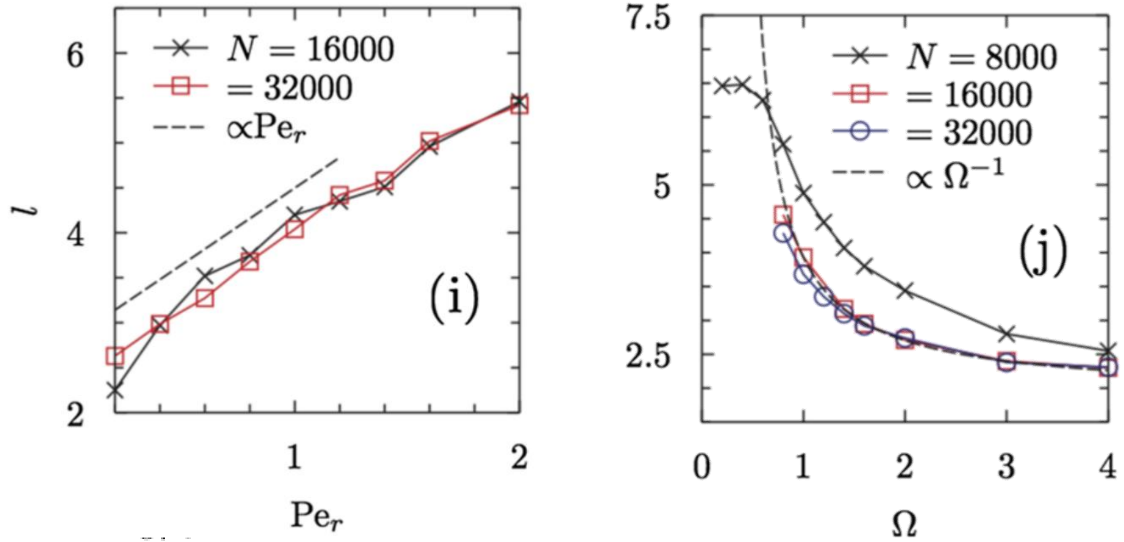

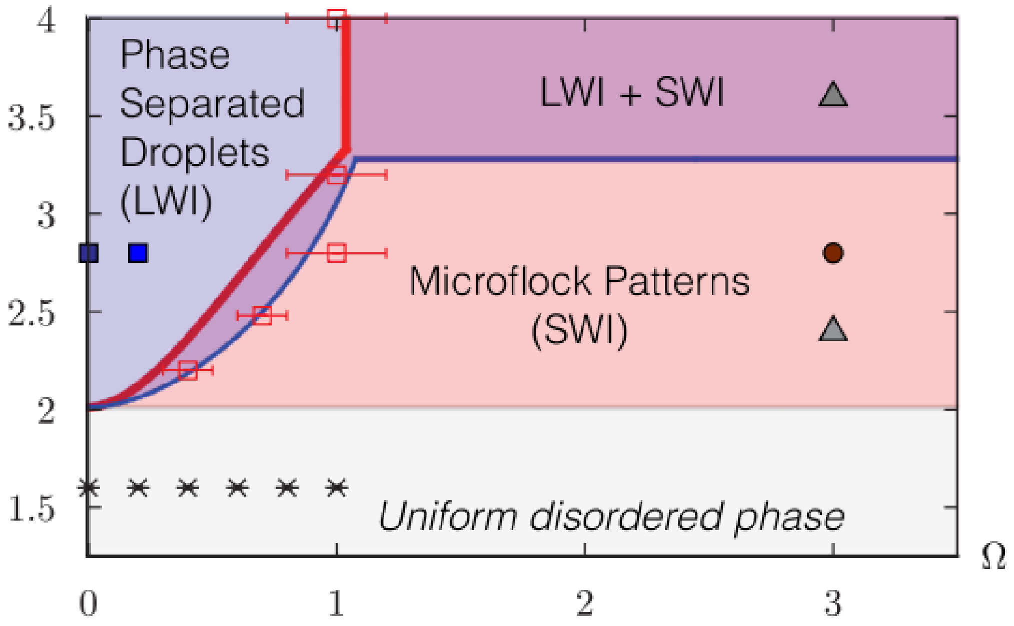

B. Liebchen and D. Levis, Collective Behavior of Chiral Active Matter: Pattern Formation and Enhanced Flocking, Phys. Rev. Lett. 119, 058002 (2017).

More CAPs Models

[1] D. Levis, I. Pagonabarraga, and B. Liebchen, *Activity Induced Synchronization: Mutual Flocking and Chiral Self-Sorting*, Phys. Rev. Research **1**, 023026 (2019).

$$\dot{\boldsymbol{r}}_\alpha = v\boldsymbol{n}_\alpha, \quad (1)$$

$$\dot{\theta}_\alpha = \omega_\alpha + \frac{K}{\pi R^2}\sum_{\nu\in\partial_\alpha}\sin(\theta_\nu - \theta_\alpha) + \sqrt{2D_r}\eta_\alpha. \quad (2)$$

[2] D. Levis and B. Liebchen, *Simultaneous Phase Separation and Pattern Formation in Chiral Active Mixtures*, Phys. Rev. E **100**, 012406 (2019).

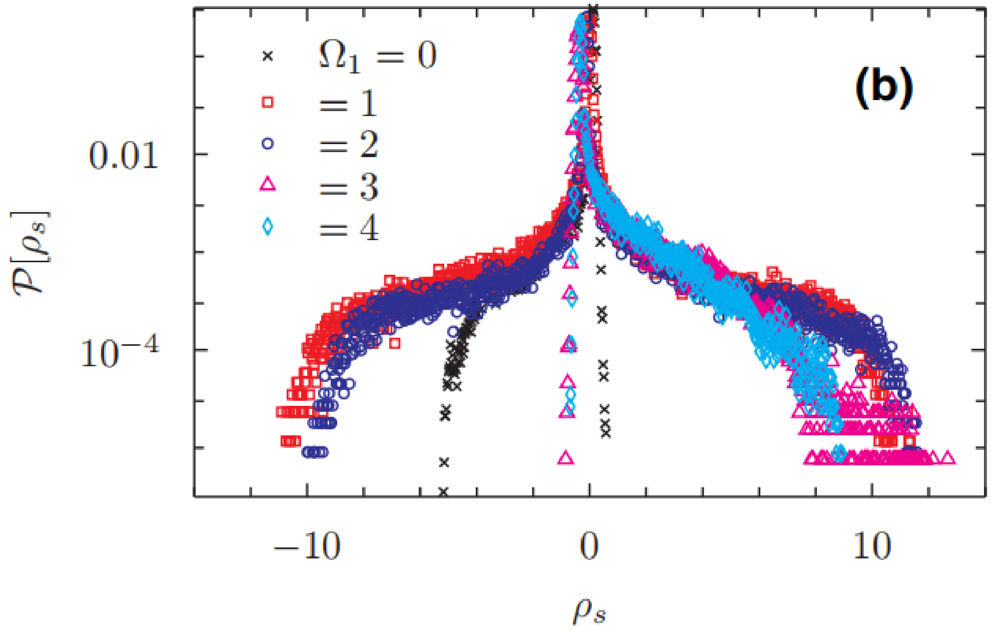

FIG. 3. Distribution of the local segregation factor $\mathscr{P}(\rho_s)$ with $\rho_s = (\rho_1 - \rho_2)/\rho_0$ for several values of Ω_1 (see key) for monochiral mixtures (fixed $\Omega_2 = 1$) (a) and for bichiral mixtures ($\Omega_2 = -1$) (b). The two dotted lines in the top panel correspond to two Gaussian distributions centered in zero with different variance.

[3] B. Ventejou, H. Chaté, R. Montagne, and X. Shi, *Susceptibility of Orientationally Ordered Active Matter to Chirality Disorder*, Phys. Rev. Lett. **127**, 238001 (2021).

$$\dot{\mathbf{r}}_i = v_0\,\mathbf{e}(\theta_i), \quad (1a)$$

$$\dot{\theta}_i = \omega_i + \kappa\langle\sin\alpha(\theta_j - \theta_i)\rangle_{j\sim i} + \sqrt{2D_r}\eta_i, \quad (1b)$$

Self-propelled chimeras

$$\dot{r}_i = \boldsymbol{v}(\varphi_i), \quad \dot{\varphi}_i = \frac{\boldsymbol{\sigma}}{|B_\rho^i|}\sum_{j \in B_\rho^i} \sin(\varphi_j - \varphi_i - \alpha),$$

$$\boldsymbol{v}(\varphi_i) = (\cos\varphi_i, \sin\varphi_i)$$

$$g(r) = \frac{1}{\pi r^2 \rho}\langle \textstyle\sum_{j(\neq i)} \delta(r - r_{ij})\rangle_i$$

$$H = \int |g(r) - 1| \mathrm{d}r$$

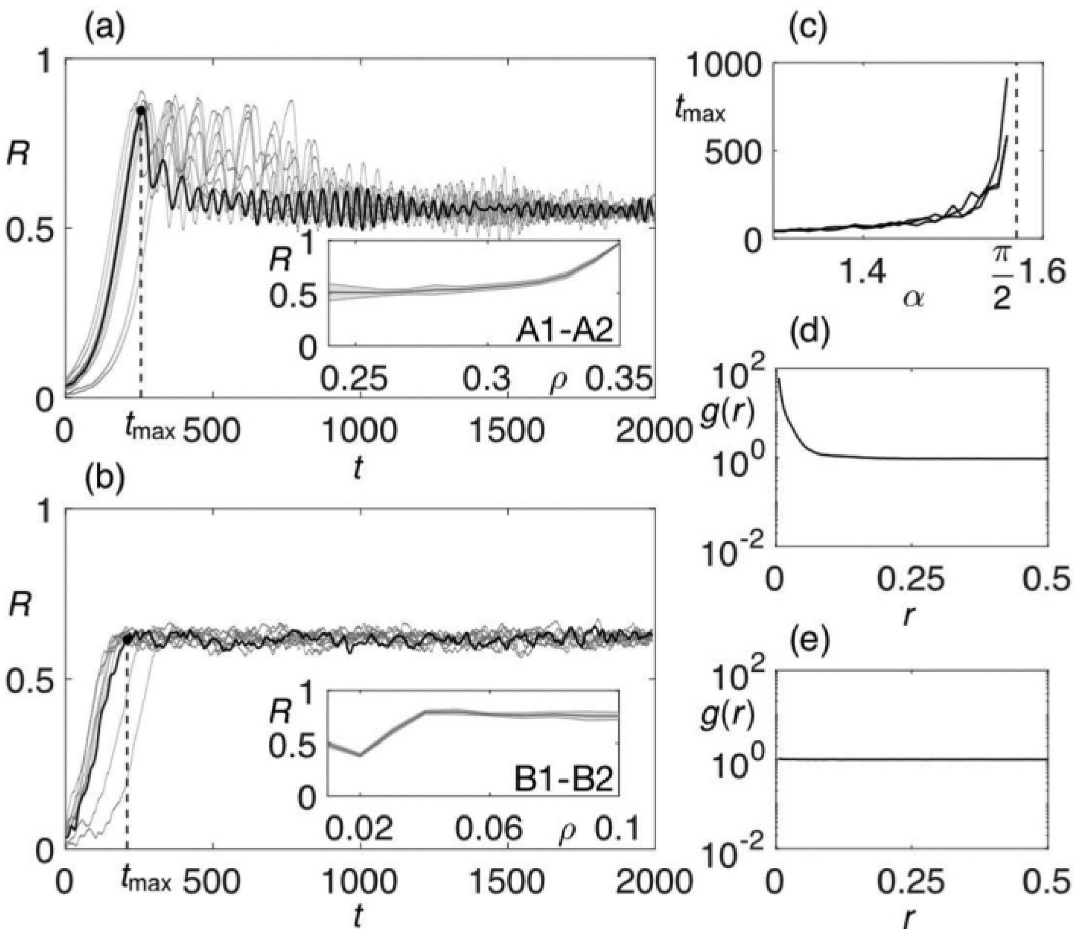

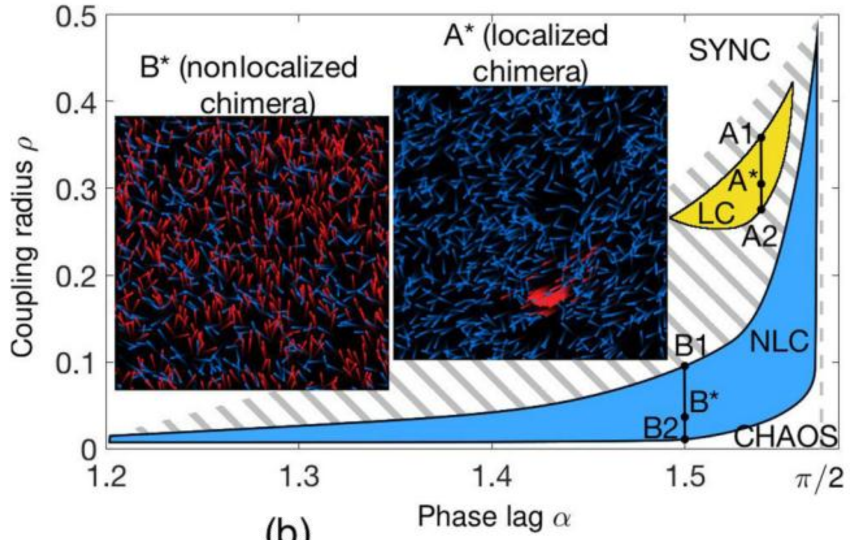

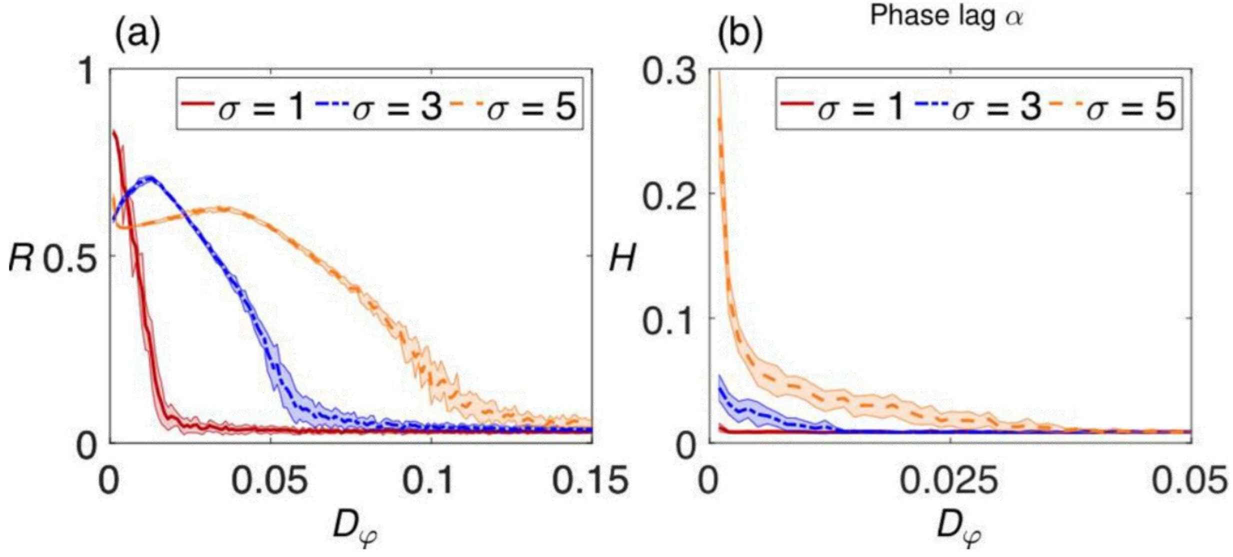

N. Kruk, Y. Maistrenko, and H. Koeppl, Self-Propelled Chimeras, Phys. Rev. E 98, 032219 (2018).

General Chemotactic Model of Oscillators

$$\dot{X}_i(t) = f(X_i) + kg(S(r_i, t)), \qquad (1)$$

$$m\ddot{r}_i(t) = -\gamma\dot{r}_i - \sigma(X_i)\nabla S|_{r=r_i}, \qquad (2)$$

$$\tau\partial_t S(r, t) = -S + d\nabla^2 S + \sum_i h(X_i)\delta(r - r_i). \qquad (3)$$

$$\dot{\psi}_i(t) = \sum_{j\neq i} e^{-|R_{ji}|}\sin(\Psi_{ji} + \alpha|R_{ji}| - c_1), \qquad (15)$$

$$\dot{r}_i(t) = c_3\sum_{j\neq i} \hat{R}_{ji}e^{-|R_{ji}|}\sin(\Psi_{ji} + \alpha|R_{ji}| - c_2), \qquad (16)$$

where $R_{ji} \equiv r_j - r_i$, $\hat{R}_{ji} \equiv R_{ji}/|R_{ji}|$, and $\Psi_{ji} \equiv \psi_j - \psi_i$. These equations contain the four real parameters $c_1 \equiv \arg(c\kappa b/\rho) - \pi/2$, $c_2 \equiv \arg(-b) - \pi/2$, $c_3 \equiv \mathrm{Re}\rho|\rho/c\kappa|(>0)$, and $\alpha \equiv \mathrm{Im}\rho/\mathrm{Re}\rho(>0)$. Note that c_3 is equal to the ratio of the time scales of ψ_i and r_i. Also, note that although the density of the elements does not appear explicitly in these equations, it is an important parameter.

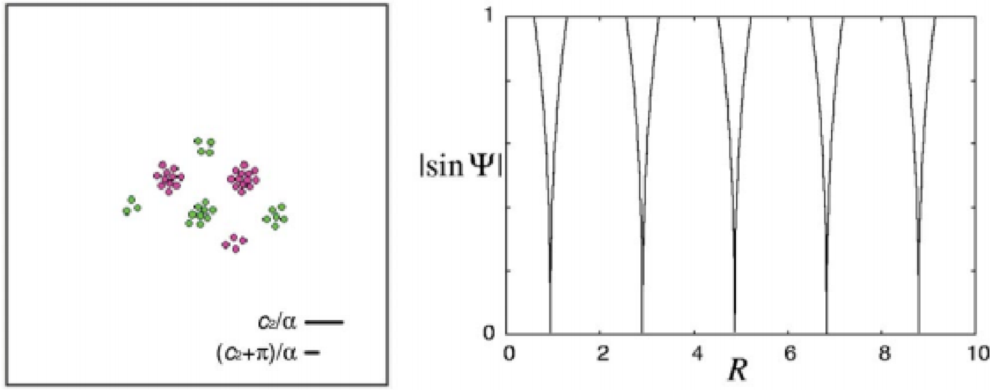

FIG. 1 (color). (left) *Clustered clusters* (or *modular networks*): snapshot of the element distribution in two-dimensional space exhibited by Eqs. (15) and (16), with $c_1 = c_2 = c_3 = 1.5$ and $\alpha = 1.6$. The colors represent the internal states ψ of the elements. The spatial size of the system is 30×30, and it is shown in its entirety. The two scale bars represent c_2/α and $(c_2 + \pi)/\alpha$ (see main text). Although we have adopted a point element in this Letter, we plot its position with a finite size to facilitate visualization. (right) Invariant curve Eq. (17) with $E = 1.3$. The parameter values are the same as above. When the oscillators synchronize, i.e. $\sin\Psi = 0$, the distance R must be approximately $1, 3, 5, \ldots$. Because $|\sin\Psi| \leq 1$, values of R in the neighborhood of $0, 2, 4, \ldots$ are avoided. In this way, an effective excluded volume (or zone) appears even though the elements are point objects.

Chemotactic Active Matter

[1] B. Liebchen, D. Marenduzzo, I. Pagonabarraga, and M. E. Cates, *Clustering and Pattern Formation in Chemorepulsive Active Colloids*, Phys. Rev. Lett. **115**, 258301 (2015).

[2] B. Liebchen, M. E. Cates, and D. Marenduzzo, *Pattern Formation in Chemically Interacting Active Rotors with Self-Propulsion*, Soft Matter **12**, 7259 (2016).

$$\dot{\rho} = -v_0 \nabla \cdot (\rho \mathbf{p}) + D_\rho \nabla^2 \rho + K \nabla^2 \rho^3 \qquad (1)$$

$$\dot{\phi} = \omega + \beta \hat{\mathbf{p}} \times \nabla c; \quad \mathbf{p} = (\cos\phi, \sin\phi)^T \qquad (2)$$

$$\dot{c} = k_0 \rho - k_\mathrm{d} c + D_\mathrm{c} \nabla^2 \mathrm{c} + \varepsilon (c_0 - c)^3. \qquad (3)$$

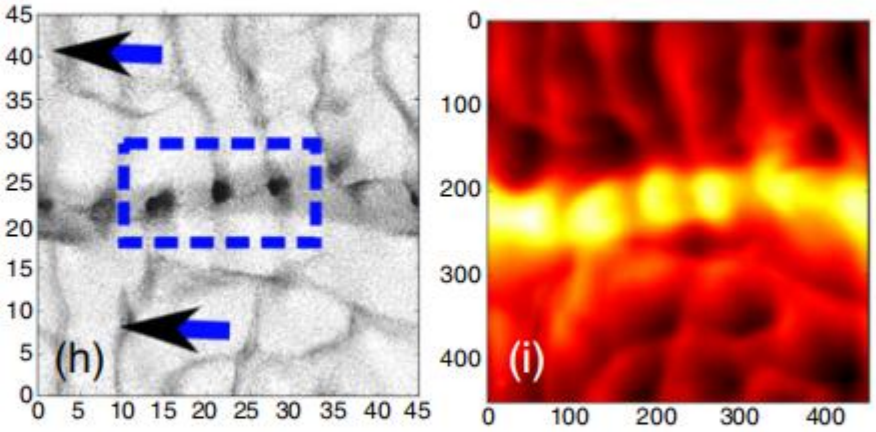

[3] B. Liebchen, D. Marenduzzo, and M. E. Cates, *Phoretic Interactions Generically Induce Dynamic Clusters and Wave Patterns in Active Colloids*, Phys. Rev. Lett. **118**, 268001 (2017).

$$\dot{\mathbf{r}}_i(t) = v \mathbf{p}_i, \qquad (1)$$

$$\dot{\theta}_i(t) = \beta \mathbf{p}_i \times \nabla c + \sqrt{2 D_r} \eta_i(t). \qquad (2)$$

$$\dot{c}(\mathbf{r}, t) = D_c \nabla^2 c - k_d c + \sum_{i=1}^{N} \oint d\mathbf{x}_i \delta(\mathbf{r} - \mathbf{r}_i(t) - R_0 \mathbf{x}_i) \sigma(\mathbf{x}_i).$$

$$\begin{aligned} \dot{\rho} &= -\mathrm{Pe} \nabla \cdot \mathbf{w}, \\ \dot{\mathbf{w}} &= -\mathbf{w} + \frac{B\rho}{2} \nabla c - \frac{\mathrm{Pe}}{2} \nabla \rho + \frac{\mathrm{Pe}^2}{16} \nabla^2 \mathbf{w} - \frac{B^2 |\nabla c|^2}{8} \mathbf{w} \\ &\quad + \frac{\mathrm{Pe} B}{16} [3 (\nabla \mathbf{w})^T \cdot \nabla c - (\nabla c \cdot \nabla) \mathbf{w} - 3 (\nabla \cdot \mathbf{w}) \nabla c], \\ \dot{c} &= \mathcal{D} \nabla^2 c + K_0 \rho + \nu \frac{K_0}{2} \nabla \cdot \mathbf{w} - K_d c. \end{aligned} \qquad (4)$$

Overview

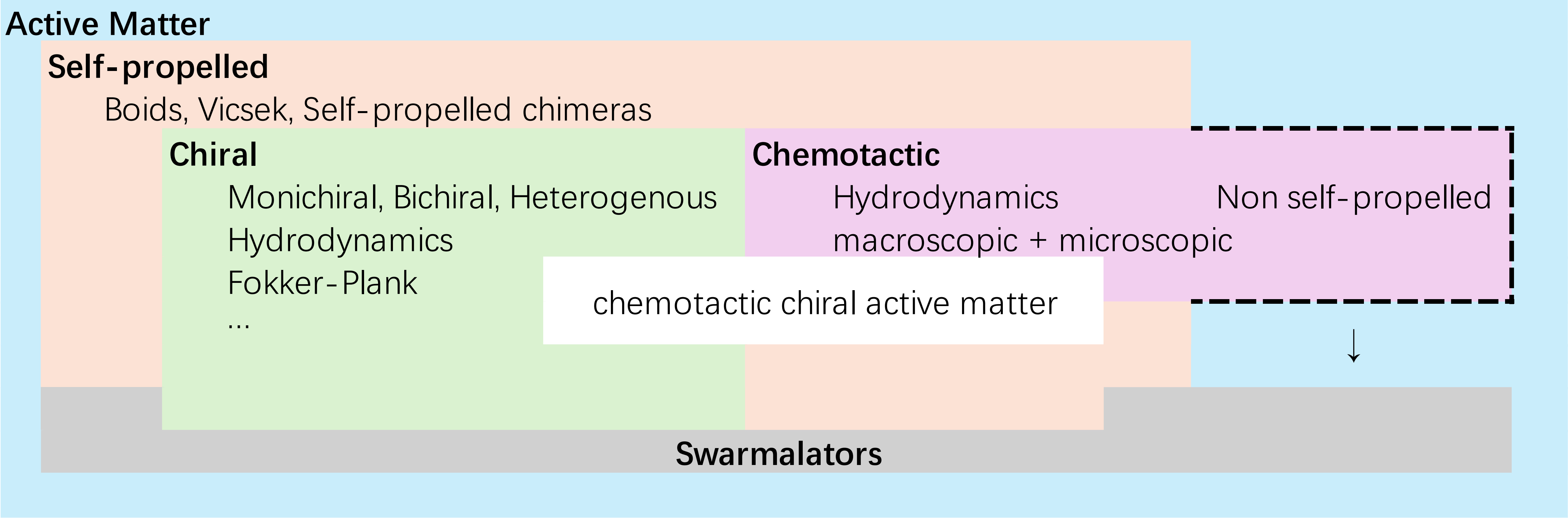
Active Matter
Self-propelled
Boids, Vicsek, Self-propelled chimeras
Chiral
Monichiral, Bichiral, Heterogenous
Hydrodynamics
Fokker-Plank
...
Chemotactic
Hydrodynamics
macroscopic + microscopic
Non self-propelled
chemotactic chiral active matter
↓
Swarmalators